

# Landmark-Aware and Part-based Ensemble Transfer Learning Network for Facial Expression Recognition from Static images

Rohan Wadhawan, *Student Member, IEEE*, Tapan K. Gandhi, *Senior Member, IEEE*

**Abstract**—Facial Expression Recognition from static images is a challenging problem in computer vision applications. Convolutional Neural Network (CNN), the state-of-the-art method for various computer vision tasks, has had limited success in predicting expressions from faces having extreme poses, illumination, and occlusion conditions. To mitigate this issue, CNNs are often accompanied by techniques like transfer, multi-task, or ensemble learning that often provide high accuracy at the cost of high computational complexity. In this work, we propose a Part-based Ensemble Transfer Learning network, which models how humans recognize facial expressions by correlating the spatial orientation pattern of the facial features with a specific expression. It consists of 5 sub-networks, in which each sub-network performs transfer learning from one of the five subsets of facial landmarks: eyebrows, eyes, nose, mouth, or jaw to expression classification. We test the proposed network on the CK+, JAFFE, and SFEW datasets, and it outperforms the benchmark for CK+ and JAFFE datasets by 0.51% and 5.34%, respectively. Additionally, it consists of a total of 1.65M model parameters and requires only  $3.28 \times 10^6$  FLOPS, which ensures computational efficiency for real-time deployment. Grad-CAM visualizations of our proposed ensemble highlight the complementary nature of its sub-networks, a key design parameter of an effective ensemble network. Lastly, cross-dataset evaluation results reveal that our proposed ensemble has a high generalization capacity. Our model trained on the SFEW Train dataset achieves an accuracy of 47.53% on the CK+ dataset, which is higher than what it achieves on the SFEW Valid dataset.

**Index Terms**—Facial Expression Recognition, Facial Landmarks Localization, Ensemble Network, Cross-Dataset Generalization, Grad-CAM, CK+, JAFFE, SFEW.

## 1 INTRODUCTION

FACIAL EXPRESSIONS play a central role in human-to-human interactions. We human beings have become adept at recognizing expressions quickly, even under challenging conditions like poor illumination, occlusion, and non-frontal poses. On the other hand, human-computer interaction is still evolving. Modern-day computers use machine learning techniques, like neural networks, to improve human-computer interaction through automated Face Detection (FD), Facial Landmark Localization (FLL), Facial Recognition (FR), and Static image or Dynamic Facial Expression Recognition. From this point onwards, we will refer to Static Image Facial Expression Recognition by the abbreviation FER.

Over the years, a large number of FER datasets have become available for training, evaluation, and benchmarking, like the Extended Cohn-Kanade (CK+) [1], Japanese Female Facial Expression (JAFFE) [2], Static Facial Expressions in the Wild (SFEW 2.0) [3], [4], Facial Expression Recognition 2013 (FER2013) [5], Real-world Affective Faces Database (RAF-DB) [6] and so on. Further, the intervention of neural networks like the Convolutional Neural Networks (CNN) has significantly improved the state-of-the-art of FER. However, vanilla CNN models have found limited success in analyzing expressions in challenging face images with varied head poses, occlusions, and illumination. To overcome this limitation, techniques like transfer, ensemble,

and multitask learning have been employed alongside CNN models to achieve high expression classification capacity.

In the case of transfer learning, one usually pre-trains FER models using an auxiliary task, or applies fine-tuning on well known pre-trained models like AlexNet [7], VGG [8], and GoogleNet [9] [10], [11]. Pre-training and fine-tuning strategies have proven to alleviate overfitting. Some techniques use a model pre-trained on large FR data like MS-1M-Celeb [12], VGGFACE2 [13], CASIA WebFace [14], and fine-tune on CK+ [1], JAFFE [2], SFEW [3] or any other FER dataset to accurately predict emotions from static images. Some researchers proposed multi-stage fine-tuning techniques over the direct use of these pre-trained models and fine-tuned models [10]. However, the representational structure of pre-trained object detection and face detection or verification models retains object or face-dominated information. This information is unrelated to emotions and may weaken the network's ability to represent emotions. For example the large domain gap with the objection net [15], and subject identification information in [11].

Network Ensemble (here it refers to the ensemble at the decision level) has outperformed individual networks to achieve high FER accuracy. A good ensemble network includes sub-networks that complement each other, combined with a suitable decision policy to predict the output [16], [17], [18], [19]. This technique, too, has its shortfall of being computationally expensive, both in time and storage, and is often challenging to implement. It is also vital to train complementary models; otherwise, an ensemble of similar models trained on the original training

• R. Wadhawan and T. K. Gandhi are with the Department of Electrical Engineering, India Institute of Technology, New Delhi, India

data may overfit unseen test data.

Multi-task FER networks are jointly trained networks. One network focuses on FER, which is the primary task. The other networks perform auxiliary tasks like AU detection, facial landmarks localization, or face recognition, which helps transfer knowledge from these secondary tasks onto the primary task [20], [21], [22], [23]. Nevertheless, this technique requires that labeled data be available for each secondary task, and the complexity of implementation increases with an increase in the number of secondary tasks.

In this paper, we synthesize the inspiration of how humans recognize expressions and the technical motivation to develop a neural architecture that is accurate, computationally efficient, and robust to challenging scenarios into a novel technique for Facial Expression Recognition. We know that human beings correlate patterns corresponding to motor movements in the facial muscles with facial expressions. From a static standpoint, we correlate the spatial orientation pattern of the various facial features like eyebrows, eyes, nose, mouth, and jaw with a corresponding emotion, in the most general case. This means that recognizing facial expressions depends upon how well an individual can detect and understand these spatial patterns. To translate this observation to the technical domain, we draw an analogy between detecting spatial patterns of facial features and FLL that predicts a fixed number of fiducial points on the face. As the change in expression, head pose, or illumination influences these points' relative position, a good FLL model must learn the representations of facial features under various expressions, poses, and illumination to accurately determine these points on the face. Thus, we fine-tune an FLL model for the task of facial expression recognition as it has already learned representations of these spatial patterns. Transfer learning from the FLL task will help the model focus on the facial feature(s) and predict expressions with high confidence. However, in real-life situations with unconstrained facial poses, the facial feature(s) this transfer learning model focuses on may be occluded, leading to misclassification. To overcome this issue, we design a part-based ensemble such that each of its sub-networks focuses on a different facial feature and makes its independent prediction. This complementarity nature of the sub-networks ensures that a misclassification by a sub-network is counteracted by the others. Complementary sub-networks also prevent the ensemble from overfitting on the training dataset. Further, we wanted to balance the trade-off between the model's computational complexity (inference time and storage requirement) and its accuracy. So, we opted for shallow neural networks to reduce the complexity.

Thus, we propose an ensemble part-based transfer learning network and perform experiments on three datasets: JAFFE, CK+, and SFEW (stands for SFEW 2.0). Here, part refers to specific facial features, like eyebrows, eyes, nose, mouth, and jaw. CK+ and JAFFE are examples of the lab-controlled dataset with a frontal head pose, and SFEW is an unconstrained dataset with varied head poses. Our proposed ensemble network performs transfer learning from the task of facial landmark localization (FLL) to facial expression recognition (FER). We use 68 fiducial points on the face and divide them into subsets of points

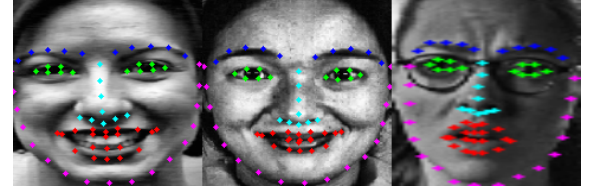


**Fig. 1:** 68 facial landmark points predicted on facial crops obtained from CK+, JAFFE, and SFEW dataset, in order left-to-right, respectively, using SSD face detection and ERT face landmark localization. Here points corresponding to eyebrows are represented by blue, eyes by green, nose by light blue, mouth by red, and jaw by pink color.

corresponding to a specific facial feature, as shown in Fig. 1. The part-based ensemble transfer learning network consists of 5 sub-networks, in which each sub-network performs transfer learning from one of the five subsets of landmarks: eyebrows, eyes, nose, mouth, or jaw. As the fiducial points on the face do not clearly distinguish between jaw, chin, and cheek area, we represent the three regions together through the sub-network jaw. The proposed approach is different from [11] as we perform transfer-learning from the task of facial landmark localization to the task of expression recognition. Unlike [20], we do not jointly train the landmark output head and classification output head. Instead, we train the landmark head first and then train the classification head along with fine-tuning the shared CNN feature extractor. Further, it is different from [10] as we do not use any external data to pre-train the network and have a single-stage fine-tuning process. Besides, our method contrasts the ensemble techniques used in [17], [18], [19] as we neither apply a hierarchical committee to ensemble individual networks nor we weigh each sub-network differently.

In addition to our proposed approach, we employ two baseline networks. These help us evaluate the benefit of transfer learning from facial landmark localization and the merit of a part-based ensemble transfer learning approach. We name the first baseline as the baseline itself and the second full transfer learning network. Moreover, to explain our model predictions, we employ Gradient-weighted Class Activation Mapping (Grad-CAM) [24] that helps visualize which regions of the face a network focuses on while performing FER. Lastly, we conduct cross-dataset generalization tests for expression classification, using which we estimate the prediction ability of the model trained and tested on two datasets having different data characteristics (like gender and ethnicity for facial data) and expression-wise distribution. Through this test, we also evaluate our model's generalizability on faces in real-world unconstrained settings, as the actual model will be deployed in similar settings. In this paper,

- We propose an ensemble part-based transfer learning neural network, which combines five shallow sub-networks in which each sub-network focuses on one facial feature - eyebrows, eyes, nose, mouth, or jaw.
- The proposed network achieves ceiling level classification performance of **97.31%** on CK+ and **97.14%** on JAFFE dataset. It has a total of **1.65M**



Fig. 2: Three original photos taken from the CK+ dataset.



Fig. 3: Three original photos taken from the JAFFE dataset.

model parameters that are lesser than the parameters of the current benchmark for all three datasets and requires only  $3.28 \times 10^6$  FLOPS. Additionally, in the worst case of serial inference, our neural model takes 6 ms on Nvidia Tesla K80 GPU and 12.5 ms on Intel Xeon CPU for predicting expression from a single face image, and consumes 25 MB of storage space.

- We employ Grad-CAM to visualize which regions of the face a network focuses on while performing FER and compare the results for the baseline, full transfer learning, and part-based ensemble transfer learning network.
- We perform a Cross-Dataset generalization test, where we use the SFEW train dataset as the training set and CK+ and JAFFE datasets for testing.

## 2 DATASETS

We use three datasets to evaluate our proposed methodology, the Extended CohnKanade (CK+) [1], Japanese Female Facial Expression (JAFFE) [2], and Static Expressions in the Wild (SFEW) [3], [4].

**CK+ dataset** is the most extensively used laboratory-controlled dataset for evaluating FER systems (some examples are shown in Fig. 2). CK+ contains 593 video sequences from 123 subjects that show a shift from a neutral facial expression to a peak expression. Among these videos, 327 sequences from 118 subjects are labeled with seven basic expression labels (anger, contempt, disgust, fear, happiness, sadness, and surprise) based on the Facial Action Coding System (FACS). We follow the protocol that uses each sequence's first frame as a neutral frame and the last three expressive frames to form our dataset, thereby obtaining 1308 images consisting of 8 expressions (7 basic + neutral) classes in total [11], [25], [26], [27], [28]. Based on the subject ID given in the dataset, we construct twelve-person subsets by sampling IDs' in ascending order and adopt a 10-fold subject-independent cross-validation strategy; each subset is used as a test set once [11], [26], [28]. The subject-independent cross-validation helps determine the generalizability of our network to novel subjects.

**JAFFE dataset** is a laboratory-controlled image dataset containing 213 samples of posed expressions from 10 Japanese females (some examples are shown in Fig. 3). Each person has 3 to 4 images across seven facial expressions: anger, disgust, fear, happiness, sadness, surprise, and neutral. The dataset is challenging because it contains a



Fig. 4: Three original photos taken from the SFEW dataset.

few examples per subject/expression. We use the leave-one-subject-out evaluation strategy [25], [29], [30], [31], [32], [33] to test our network's generalizability to novel subjects. In this strategy, we train a model in a subject-independent manner using images belonging to nine out of the ten subjects and test it on the remaining subject's images and repeat the entire process ten times. The average performance across the ten models is a good indicator of the proposed method's ability to classify facial expressions.

**SFEW 2.0 dataset** is the most widely used benchmark dataset for facial expression recognition in the wild. It provides 1,766 images, comprising 958 train, 436 validation, and 372 test images. Each of the images belongs to one of seven expression classes, i.e., anger, disgust, fear, neutral, happy, sad, and surprise. These images have varied head pose(yaw, bobble, and pitch), facial sizes, and contrast, as shown in Fig. 4. Moreover, the dataset curators provide train and validation sets' expression labels while holding the test set labels back for the EmotiW 2015 challenge [34]. Thus, we report our performance on the validation set for comparison with other methods [11], [26], [35], [36], [37].

## 3 METHODOLOGY

Our Facial Expression Recognition pipeline consists of 7 stages: Input, Image Contrast Enhancement, Face Detection, Landmark Ground-truth Annotation, Data Augmentation, Neural Network Training, and Expression Prediction, as shown in Fig. 5. All the seven stages of the entire FER pipeline are described in detail in the following subsections.

### 3.1 Input Image

We use grayscale images in all the experiments. The grayscale channel is repeated thrice for each image and concatenated to produce a three-channel image as required further down the pipeline. Then, we resize each image to 300x300x3 using bilinear interpolation before feeding it to the face detector (the number of channels has been empirically determined). Any subsequent rescaling of the image also uses bilinear interpolation for consistency.

### 3.2 Image Pre-Processing

Image Pre-Processing image accounts for three stages in the pipeline, namely - Image Contrast Enhancement, Face Detection, and Landmark Ground-truth Annotation. We use Contrast Limited Adaptive Histogram Equalization (CLAHE) [38] to perform contrast enhancement of all images across all three datasets. After contrast enhancement, we apply OpenCV's SSD detector [39], [40] on the images and obtain facial crops from it based on the bounding box predicted by the detector. Then, we resize each face crop to the size 160x160x3, as this is the input size expected by the neural network. Then, we move

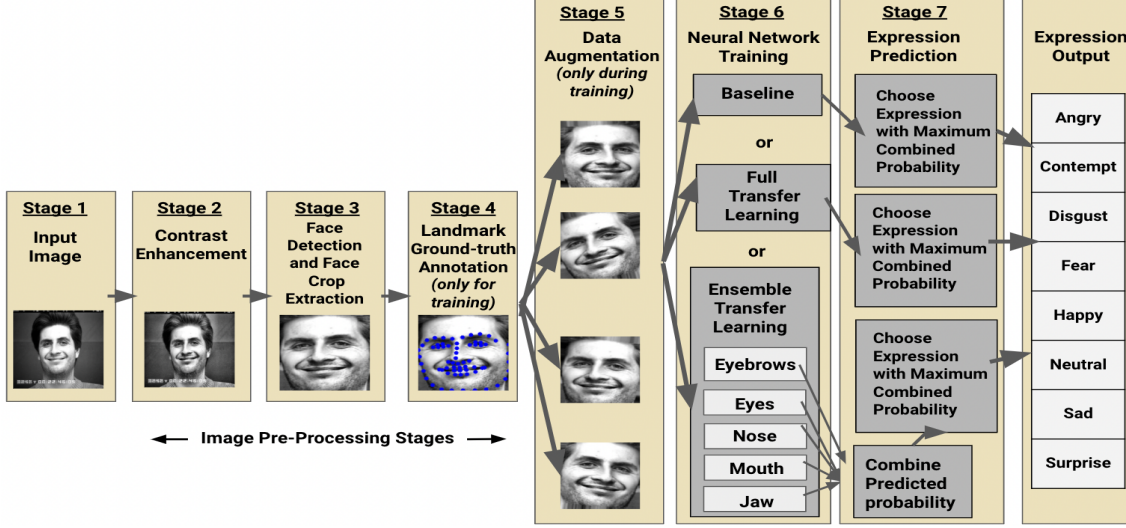


**Fig. 5:** The Seven Stages of our Facial Expression Recognition Pipeline. The landmark ground-truth annotation and data augmentation stages are used only during training. Here, the expression *Contempt* is applicable only for the CK+ dataset.

to the Facial Landmark Ground-truth Annotation Stage. Our approach performs transfer learning from the task of FLL to expression classification. FLL training gives rise to the need for annotated data for facial landmarks in addition to expression labels. However, FER datasets either do not have landmark annotations, or these annotations differ in the number of landmarks annotated, method of annotation (manual or automated), and the choice of automated annotation algorithm. CK+ dataset provides 68 landmark position annotations for each image that are Active Appearance Model (AAM) tracked [41], [42]. JAFFE dataset does not provide landmark annotation. Lastly, the SFEW dataset uses a different AAM implementation [43] for annotating the landmark positions. Moreover, the number of landmark positions differs among SFEW images; some have 39, and others have 68 positions annotated. Therefore, we need a uniform method to annotate ground truth landmark positions across all datasets. Further, we do not intend to make a highly precise model for FLL, as its goal is to guide expression classification. Thus, we allow for small precision errors in the annotation of the ground truth landmark positions. Consequently, we choose Dlib’s Ensemble Regression of Trees (ERT) model [44] for automated annotation to obtain 68 landmark position ground-truth data. We use this data to train our network’s landmark localization head, as shown in Fig. 1. This ERT model has been trained on the iBUG 300-W face landmark [45]. A detailed analysis of the choice of contrast enhancement, face detection, and landmark ground-truth annotation method employed in our FER pipeline is provided in Appendix A.

### 3.3 Neural Network Architecture

This section describes our part-based ensemble transfer learning network and two baseline networks for comparison. Each of the FER networks mentioned above consists of two or all of these parts: CNN Feature Extractor, Landmarks Localization head, and Expression Classification head, as shown in Fig. 6. The first baseline network, called Baseline Network, comprises of CNN feature extractor

and the classification head. This baseline network aims to compare the performance of non-transfer learning with the transfer learning networks. The second baseline network, called the Full Transfer Learning network, consists of a CNN feature extractor, a Landmark localization head, and a classification head. In this case, the landmark localization head is trained to predict all 68 fiducial points at once. Further, the feature extractor is shared between the localization and the classification heads. This second baseline network aims to comparatively evaluate the part-based ensemble and the full transfer learning network. Lastly, our proposed Part-Based Ensemble Transfer Learning Network comprises five transfer learning networks, such that each one focuses on one of the following facial features: eyebrows, eyes, nose, mouth, and jaw. Here, the jaw sub-network represents three regions of the face: jaw, chin, and cheek. During the landmark localization training phase, each sub-network predicts a subset of the 68 fiducial points corresponding to one of the five features mentioned above, such that the union of all these subsets is the entire set of points. Like the full transfer learning network, the feature extractor is shared between the localization and the classification heads for each sub-network.

**CNN Feature Extractor** consists of a sequence of 4 Convolutional Blocks and Max Pooling layer pairs arranged alternatively, followed by a Global Average Pooling layer. Each convolutional block, in turn, consists of two convolution and two batch normalization layers arranged alternately. After each batch normalization layer, we apply the RELU [46] activation. Batch normalization [47] enables faster and more stable training of the network. Further, we initialize each convolution layer using He uniform initializer [48]. The feature extractor’s input is a grayscale face crop of  $160 \times 160 \times 3$ , and the output is a 128-dimensional (128-D) feature vector. The feature extractor has about 0.29 M (million) parameters. Its architecture is the same across all three datasets and the three types of networks (baseline, full transfer learning, and part-based

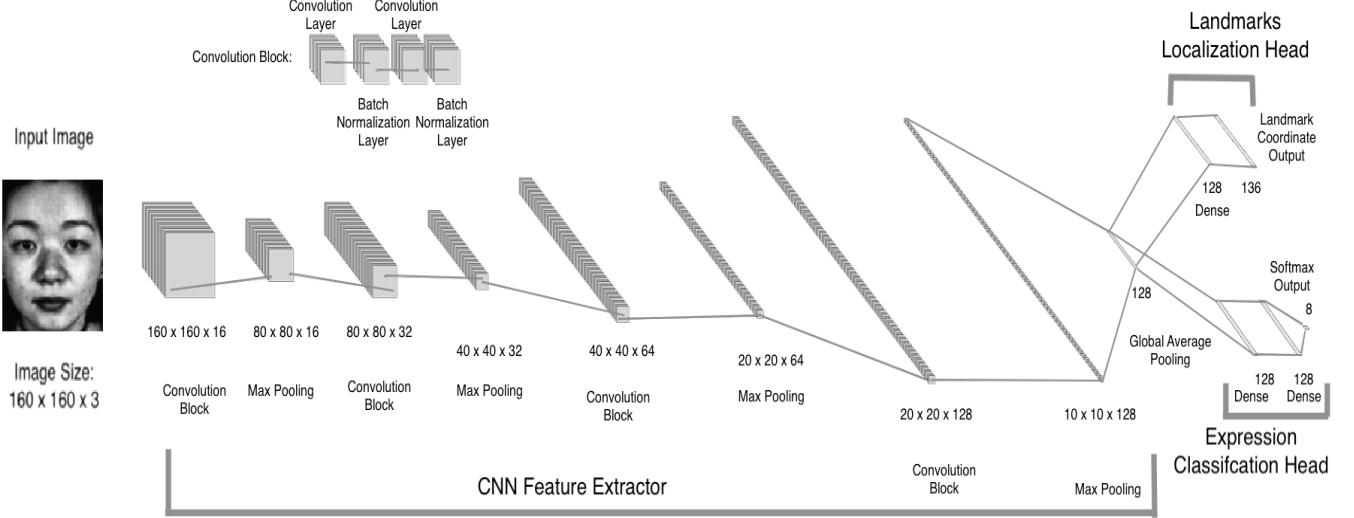


**Fig. 6:** Our FER network consists of three parts - Feature extractor, Landmarks Localization head, and Expression Classification Head. (Here, maximum landmark outputs vary from a minimum of 18 for 9 nose points to 136 for the entire 68 points, and the expression output size is 7 for JAFFE and SFEW and 8 for CK+ because of extra expression *Contempt*).

ensemble transfer learning).

**Landmarks Localization Output Head** takes the 128-D feature vector as input and consists of two dense layers. We initialize each dense layer using the Glorot uniform initializer [49]. The first dense layer is 128-D in size, and the second is the output layer with a size that varies depending on the model. The full transfer learning network learns the 68 landmark points represented by 136 output neurons. However, we divide these 68 landmarks into five sets for the ensemble network, each corresponding to a specific facial feature: eyebrows, eyes, nose, mouth, and jaw, in the order of a top to bottom vertical face scan. We then train an FLL model for each feature, thereby training 5 FLL models in total for one ensemble network. The outputs of these five models are; 20 neurons representing the 10 eyebrows points, 24 neurons representing the 12 eyes points, 18 neurons representing the 9 nose points, 40 neurons representing the 20 mouth points, and 34 neurons representing the 17 jaw points. Consequently, the number of localization head parameters varies from 0.019M for the 9 nose points to 0.025M for the entire 68 points.

**Expression Classification Output Head** takes the 128-D feature vector as input and consists of 3 dense layers. We initialize each dense layer using the Glorot uniform initializer. The first two are 128-dimensional layers, and the last one is an output layer of 7 or 8 neurons. JAFFE and SFEW datasets have labeled data for seven expressions, whereas the CK+ dataset has the expression label *Contempt* and these seven expressions. The activation for the output neurons is softmax. The Classification head of the models trained on JAFFE, SFEW, and CK+ have approximately 0.035M parameters (maximum in CK+ because it has eight output neurons).

### 3.4 Training process

In the case of the baseline network, we directly train it on the expression datasets without performing transfer learning. On the other hand, we divide the training process into

two parts for the full and part-based ensemble transfer learning networks. Firstly, we train the facial landmark localization head and the feature extractor. Then, we train the expression classification head and fine-tune the feature extractor shared with the localization head. We apply this training strategy for both full and part-based ensemble transfer learning networks. Subsequently, we obtain one expression classification model for the full transfer learning network and five expression models for the ensemble transfer learning network, one for each facial feature. To ensure a consistent comparison between our proposed ensemble and the two baseline networks, we train five model ensembles for baseline and full transfer learning networks. Furthermore, each model is trained on one dataset only. For instance, the SFEW dataset model has only seen the SFEW training dataset's images. We do not pre-train our feature extractors on any other FER or face dataset.

Before training the models, we perform data augmentation like horizontal flipping, rotation, shear, and translation to increase the training data's size, as shown in Fig. 5 and normalize input between  $[-1, 1]$ . The landmark coordinates undergo the same transformations as their corresponding images for training the localization head. After transformation, we normalize the landmark coordinates between  $[0, 1]$ . We train the neural network using backpropagation techniques and formulate two losses: facial landmark localization and the other for expression classification. For each training image sample  $x_i$ , we have

**Facial Landmark Localization Training**, which is formulated as a regression problem where we minimize the L1 loss:

$$L_1 = |y_i - \hat{y}_i| \quad (1)$$

where  $y_i \in [0, 1]^z$  is the ground truth coordinate for the  $i$ -th sample and  $\hat{y}_i \in [0, 1]^z$  is the coordinate predicted by the network and  $z \in \{18, 20, 24, 34, 40, 136\}$  represents the number of output neurons based on the landmarks model being trained.

**Expression Classification Training**, which is formulated as 7 or 8 class classification problem where we minimize the categorical crossentropy loss:

$$\text{Categorical Cross Entropy} = -\log \left( \frac{e^{s_p}}{\sum_j^C e^{s_j}} \right) \quad (2)$$

Where  $s_p$  is the score of the positive class,  $s_j$  is the score of the class  $j$ ,  $C$  is the number of classes,  $\text{Classes} = \{\text{Angry}, \text{Contempt}^*, \text{Disgust}, \text{Fear}, \text{Happy}, \text{Neutral}, \text{Sad}, \text{Surprise}\}$ , (\*Contempt only in CK+)

Furthermore, neural network weights are optimized using Adam optimizer [50]. In the baseline network's case, we use an initial learning rate  $\alpha = 0.01$  for training the model. For the full transfer learning and each sub-network of the part-based ensemble transfer learning network, we use an initial learning rate of  $\alpha = 0.01$  for training the localization head and the feature extractor, followed by an initial learning rate of  $\alpha = 0.0001$  for the training the classification head and fine-tuning the feature extractor. Other optimizer parameters, that is,  $\{\beta_1 = 0.9, \beta_2 = 0.999, \epsilon = 10^{-7}\}$  and a mini-batch size of 32 images, are kept the same for each network. We stop training a model when the validation loss saturates. As validation loss saturation is different for models trained on the three datasets, the average number of epochs a model is trained for varies. While training the models trained on each of the three datasets, we keep the hyperparameter values consistent, but the number of epochs may differ.

**Training Environment** We use Tensorflow, and Keras deep learning framework to train our models and train them on a single Nvidia Tesla K80 GPU.

### 3.5 Inferencing

We exclude the landmark localization head (if applicable) and fix the model weights learned during training.

**Ensemble Prediction Policy** states how we predict the classification outcome from the ensemble transfer learning neural network's output. Each network outputs a vector of probabilities between 0 and 1 of length  $C$  (number of classes). We perform expression-wise summation of these probabilities to get a final output vector and use it for prediction, as shown below:

$$\text{Predicted Label}_{(\text{ensemble})} = \arg \max_k \sum_m \text{Prob}(s) \quad (3)$$

Where  $m \in \{\text{eyebrows}, \text{eyes}, \text{nose}, \text{mouth}, \text{jaw}\}$  model,  $s$  stands for score,  $k \in \text{Classes}$ ,  $\text{Prob}(s) \in [0, 1]^C$

**Inference Environment** We perform inferencing on a single Nvidia Tesla K80 GPU and Intel(R) Xeon(R) CPU @ 2.20GHz.

## 4 RESULTS

### 4.1 Benchmark Dataset Analysis

In this section, we present the baseline, full and part-based ensemble learning network results for the three datasets - CK+, JAFFE, and SFEW (as shown in Table 1) and compare

them with the current benchmark (as shown in Table 2). We report each network's average expression classification accuracy in Table 1. We also report the accuracy of each sub-network of the ensemble network when it is used independently. For a fair comparison with the part-based ensemble transfer learning network, we train 5-model ensembles of both the baseline and full transfer learning (as mentioned in Section 3.4) and report their classification accuracies for each of the three datasets. Moreover, in Table 2, we compare our proposed ensemble network's accuracy and model parameter count with the current benchmark for the three datasets, whose values are taken from the respective papers. As the highest decimal precision of the reported accuracy values for the current benchmark results across all three datasets is two decimal places, we round off our accuracy values accordingly.

We only present the benchmark results for each dataset in Table 2 for the sake of conciseness and clarity. Nevertheless, we compare our network's performance against other comparable research work. By comparable, we mean prior work which has the following characteristics: same version of the dataset as us (for example, SFEW 2.0 and not SFEW 1.0 dataset); the same evaluation policy (10-fold subject independent evaluation for CK+ and JAFFE dataset, and validation dataset evaluation for SFEW) as us; no pre-training on any other FER or FR dataset; evaluating the result for seven expression classes for JAFFE and SFEW, and eight expression classes for CK+ datasets. Thus, we compare our results with the following prior works: [11], [26], [28] for CK+, [25], [29], [30], [31], [32], [33] for JAFFE, and [11], [26], [35], [36], [37] for SFEW. Lastly, we also illustrate confusion matrices to analyze the part-based ensemble transfer learning network's expression-wise accuracy. For CK+ and JAFFE (Fig. 7 and Fig. 8 respectively), the confusion matrix is the summation of the ten confusion matrices, one for each subject independent cross-validation fold. In the case of SFEW, we construct the confusion matrix by evaluating our proposed ensemble network on the SFEW validation dataset, as shown in Fig. 9.

#### 4.1.1 CK+ dataset

We train each baseline model for 400 epochs. Further, we train the feature extractor and the localization head of the full transfer learning and each sub-network of the part-based ensemble transfer learning network for 100 epochs. We then fix the localization head, train the classification head, and fine-tune the feature extractor for 300 epochs. This training strategy and fine-tuning strategy are applied five times for each sub-network of the ensemble network. The average accuracy over the ten subject independent folds for the baseline, full transfer learning, and ensemble transfer learning network is shown in Table 1.

#### 4.1.2 JAFFE dataset

We train each baseline model for 300 epochs. Further, we train the feature extractor and the localization head of the full and the sub-networks of the ensemble transfer learning network for 100 epochs. We then fix the localization head, train the classification head, and fine-tune the feature extractor for 200 epochs. Like the CK+ dataset, this training strategy and fine-tuning strategy are applied five times for

**TABLE 1:** Accuracy of expression classification of the Baseline, FTL: Full Transfer Learning and EL: Part-based Ensemble Transfer Learning networks.

Dataset	Classification Accuracies (%) of Neural Networks								
	Baseline	FTL	Individual EL					EL	
			Eyebrows	Eyes	Nose	Mouth	Jaw		
CK+	82.56	95.87	93.29	93.96	91.86	95.16	93.28	<b>97.31</b>	
JAFFE	85.02	92.42	91.43	87.30	82.88	92.36	86.40	<b>97.14</b>	
SFEW	36.47	42.20	36.70	41.30	40.60	41.74	40.82	<b>44.50</b>	

**TABLE 2:** Comparison of EL: Part-based Ensemble Transfer Learning Network with CB: Current Benchmark on the basis of Classification Accuracy and Model Parameters.

Dataset	Classification Accuracies (%)		Model Parameters (M)	
	CB	EL	CB	EL
CK+	96.80 [11]	<b>97.31</b>	11	<b>1.65</b>
JAFFE	91.80 [25], [51]	<b>97.14</b>	2	<b>1.65</b>
SFEW	<b>48.19</b> [11]	44.50	11	<b>1.65</b>

each sub-network of the ensemble network. The average accuracy over the ten subject independent folds for the baseline, full transfer learning, and ensemble transfer learning network is shown in Table 1.

#### 4.1.3 SFEW dataset

We use 940 out of 958 images from the SFEW train dataset because the SSD face detector cannot detect the remaining 18 images. However, we use the entire validation dataset consisting of 436 images to report our results. Thus, our results are comparable to those methodologies that use the entire validation dataset. We train each baseline model for 400 epochs. Further, we train the feature extractor and the localization head of the full and the sub-networks of the ensemble transfer learning network for 200 epochs. We then fix the localization head, train the classification head, and fine-tune the feature extractor for 200 epochs.

From Table 1, we can infer that on keeping the feature extractor and classification head networks’ architecture constant, the transfer learning from facial landmark localization technique is better than the vanilla CNN-based expression classification technique. The part-based ensemble transfer learning method outperforms the 5-model ensembles of both the full transfer learning and baseline networks. We also observe that the full transfer learning network, which learned to localize all 68 fiducial points, performs better than sub-networks of our proposed ensemble that only learn to localize a subset of those points corresponding to a specific facial feature. This demonstrates that transfer learning from one facial feature is not sufficient to predict expressions with high confidence. However, on combining individual networks, where each transfer learns from a different feature, we obtain an ensemble that outperforms an ensemble of networks, where each transfer learns from all the features (shown in Table 1. This validates a key design parameter of complementary sub-networks for our proposed ensemble.

Furthermore, the sub-network focussing on the mouth region has the highest independent classification accuracy.

Actual	Angry	Contempt	Disgust	Fear	Happy	Neutral	Sad	Surprise	Predicted	
									Angry	Contempt
Angry	132	0	0	0	0	0	0	0	3	0
Contempt	0	48	0	0	0	0	0	0	6	0
Disgust	0	0	177	0	0	0	0	0	0	0
Fear	0	0	0	66	0	0	3	3	3	3
Happy	0	0	0	0	207	0	0	0	0	0
Neutral	1	0	0	0	0	326	0	0	0	0
Sad	0	0	0	0	0	10	74	0	0	0
Surprise	0	3	1	0	0	3	0	242	0	0

**Fig. 7:** Confusion matrix for the proposed ensemble network’s results on all the ten validation folds of the CK+ dataset.

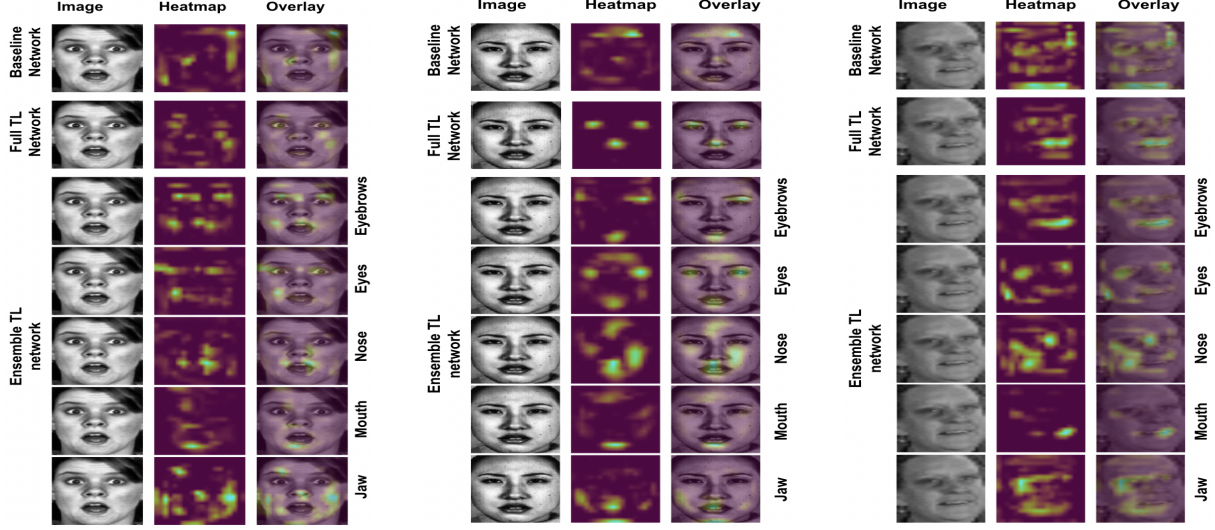
Actual	Angry	Disgust	Fear	Happy	Neutral	Sad	Surprise	Predicted		
								Angry	Disgust	
Angry	29	0	0	0	0	1	0	0	0	0
Disgust	0	29	0	0	0	0	0	0	0	0
Fear	0	0	32	0	0	0	0	0	0	0
Happy	0	0	0	30	0	0	0	0	0	1
Neutral	0	0	0	0	30	1	0	0	0	0
Sad	0	1	0	1	0	29	0	0	0	0
Surprise	0	0	0	1	0	0	29	0	0	0

**Fig. 8:** Confusion matrix for the proposed ensemble network’s results on all the ten validation folds of the JAFFE dataset.

Actual	Angry	Disgust	Fear	Happy	Neutral	Sad	Surprise	Predicted		
								Angry	Disgust	
Angry	32	3	3	9	13	7	10	0	0	0
Disgust	3	1	1	5	6	5	2	0	0	0
Fear	13	2	1	7	9	10	5	0	0	0
Happy	3	0	1	54	4	10	1	0	0	0
Neutral	5	2	3	2	56	15	3	0	0	0
Sad	0	0	2	3	19	41	8	0	0	0
Surprise	7	0	0	6	26	9	9	0	0	0

**Fig. 9:** Confusion matrix for the proposed ensemble network’s results on the validation set of the SFEW dataset.

After the mouth region, eyes and eyebrows have the



(a) CK+ image with *Surprise* expression. (b) JAFFE image with *Disgust* expression. (c) SFEW image with *Happy* expression.

**Fig. 10:** Grad-CAM visualization of the Baseline network, Full Transfer Learning network, and each sub-network of the Part-based Ensemble Transfer Learning network for a given expression.

second-highest independent classification accuracy, which is further followed by jaw and nose (with the nose having the least). Now, we try to relate these findings with the Facial Action Coding System (FACS) Main Action units (AUs) and how they are combined to describe emotions - anger, disgust, fear, happiness, sadness, and surprise. We find that action units corresponding to the mouth region (lip movement) produce the most diverse visual variations. Further, the lip AUs used to describe the expressions are often unique and specific to an expression. Then, we have the AUs describing the eyes (eyelid movement) and eyebrows (brow movement), which produce the second most visual variations. Unlike lip AUs, eyelid and brow AUs are often the same across different expressions. We consider cheek, chin, and jaw AUs together to draw correspondence with our proposed ensemble's jaw sub-network. Like eyelid and brow, these AUs are often the same across expressions, but they are used in fewer expressions than even eyelid and brow AUs. Lastly, only one nose AU is used to describe an expression, which is disgust. As expression classification from static images is a pattern recognition problem, higher discriminability of patterns corresponds to higher classification accuracy. From the above discussion on AUs, we obtain the following order of discriminability - mouth, eyes, eyebrows (similar in magnitude to eyes), jaw, and nose. This order conforms with the results we have obtained (as discussed above), thereby demonstrating that our model can correlate the visual patterns emanating from facial muscles' motor movements to emotions, a key design parameter for our network.

Moreover, we compare our proposed part-based ensemble's results with the three datasets' current benchmarks. We observe that our proposed ensemble obtains the highest reported accuracy of 97.31% for CK+ and 97.14% for JAFFE (subject to evaluation criteria), outperforming the benchmark for CK+ by 0.51 %, and Jaffe by 5.34%, as shown in Table 2. It falls short of the benchmark for SFEW by 3.69 %, but has nearly 1/7th

the total model parameters compared to the benchmark network. Moreover, our network consistently has a lesser number of total model parameters than the benchmarks. We know that a model's training time and storage space depend on model (trainable + non-trainable) parameters. This means that our proposed ensemble model, which has lesser model parameters than the current benchmarks, is more computationally efficient. Thus, our part-based ensemble transfer learning network performs a good trade-off between accuracy and computational efficiency, another key design parameter for our network.

Furthermore, the confusion matrices reveal information about the underlying expression-wise distribution of the three datasets. CK+ and SFEW datasets have an imbalanced expression-wise distribution. This imbalance is evident in Fig. 7 and in Fig. 9, where the maximum false positives are for the class neutral, which happens to be the most prevalent class in both the datasets. On the contrary, the JAFFE dataset, a nearly balanced expression-wise dataset, has no such prediction bias for a single expression class (shown in Fig. 8).

## 4.2 Explaining expression prediction through Grad-CAM visualization

To interpret how the different convolutional sub-networks of the ensemble network work, we employ Gradient-weighted Class Activation Mapping (Grad-CAM) [24]. Grad-CAM uses the gradient information flowing into the last convolutional layer of CNN to understand each neuron for a class label of interest. We obtain the class discriminative localization map of width  $u$  and height  $v$  for any expression class  $c$  by first computing the gradient of the score for that class, that is,  $y^c$  (before the softmax), for feature maps  $\alpha_k$  of a convolutional layer. These gradients flowing back are global average-pooled over the width and height dimensions (indexed by  $i$  and  $j$  respectively) to obtain the

**TABLE 3:** Cross-Dataset Generalization test of the Baseline, FTL: Full Transfer Learning and EL: Part-based Ensemble Transfer Learning networks from SFEW Train dataset to CK+ and JAFFE datasets.

Train Dataset	Test Dataset	Classification Accuracies (%) of Neural Models								
		Baseline	FTL	Individual EL					EL	
				Eyebrows	Eyes	Nose	Mouth	Jaw		
SFEW Train	SFEW Valid	36.47	42.20	40.82	41.30	36.70	41.74	40.60	44.50	
SFEW Train	CK+	32.85	41.31	33.33	35.49	22.97	37.72	32.62	<b>47.53</b>	
SFEW Train	JAFFE	16.90	26.29	22.54	24.88	18.78	24.88	21.60	30.51	

neuron importance weights  $\alpha_k^c$ .

$$\alpha_k^c = \underbrace{\frac{1}{Z} \sum_i \sum_j}_{\text{global average pooling}} \underbrace{\frac{\partial y^c}{\partial A_{ij}^k}}_{\text{gradients via backprop}} \quad (4)$$

After calculating  $\alpha_k^c$ , we perform a weighted combination of the activation maps and follow it by a ReLU. Without it, the class activation map highlights more than required and achieves low localization performance.

$$L_{\text{Grad-CAM}}^c = \text{ReLU} \left( \underbrace{\sum_k \alpha_k^c A^k}_{\text{linear combination}} \right) \quad (5)$$

Subsequently, we superimpose the activation map (heatmap) with the original image to coarsely visualize which region of the face each sub-network of our proposed ensemble focuses on while performing FER. We use a 5-model ensemble for both the baseline and full transfer learning network to ensure a fair comparison with our part-based ensemble. Thus, the final heatmap of baseline and full transfer learning network (as shown in Fig. 10) results from the union of 5 heatmaps. Subsequently, the final heatmap is superimposed on the image to get the overlap map.

The heatmap and overlap maps for the baseline network in Fig 10 show that the network does not focus on facial features specifically. Instead, it is trying to find a pattern from the entire face. On the other hand, Fig. 10 demonstrates that transfer learning from the FLL task helps the Full Transfer Learning network focus on facial features, which uses this ability for expression prediction. In Fig 10a the full transfer learning network focuses on the eyes, eyebrows, and jaw to detect the expression of surprise; in Fig 10b it focuses on the eyes and nose to detect the expression of disgust; in Fig 10c it focuses on the eyes and mouth to detect the expression happy. Lastly, we visualize our proposed ensemble network. From the heatmaps and overlay maps, we observe that each sub-network focuses on one facial feature to make its independent expression prediction, which is later combined using the ensemble prediction policy. These visualizations demonstrate the complementary nature of our ensemble’s sub-networks, a critical parameter for a successful ensemble network.

### 4.3 Cross-Dataset Generalization

In cross-dataset generalization tests, we estimate the expression prediction ability of the model trained and tested

on two datasets having different data characteristics and expression-wise distribution. A cross-dataset generalization test result is good if it approaches the given model’s accuracy on a test dataset belonging to the same distribution as the one on which it is trained. Through this test, we also evaluate our model’s generalizability on faces in real-world unconstrained settings, as the actual model will be deployed in similar settings. We know that the SFEW dataset consists of facial images with varied poses, sizes, and facial expressions. In other words, these images can be taken as a good approximation of faces a model will encounter in the wild. Whereas the lab-controlled CK+ and JAFFE datasets consist of fewer subjects and consist of only faces with frontal poses, thereby representing an ideal condition for facial expression analysis, not a generalized one.

Therefore, we perform a Cross-Dataset generalization test, where we use the SFEW train dataset as the training set and CK+ and JAFFE datasets for testing. While testing on the CK+ dataset, we drop the samples whose expression class is Contempt as this class is absent in the SFEW dataset. We perform this test for each network type - baseline, full transfer learning, and part-based transfer learning. For baseline and full transfer learning networks, we use 5-model ensembles trained on SFEW (train) dataset to ensure a fair comparison with our proposed 5-part ensemble model trained on the same dataset. We also report the independent generalization ability of each sub-network of the proposed ensemble, as shown in Table 3.

From Table 3, we observe that the classification accuracy achieved by all three networks on the CK+ dataset is at par with those achieved on the SFEW Valid dataset. Moreover, the part-based ensemble achieves an accuracy of 47.53% on the CK+ dataset, which is even higher accuracy than the accuracy it obtains on the SFEW valid dataset. This shows that our proposed ensemble shows high generalization from SFEW to the CK+ dataset. On the other hand, the level of generalization from SFEW to JAFFE is comparatively less. This can be attributed to the dataset properties like gender and ethnicity covered in the datasets’ images. Both SFEW and CK+ datasets consist of multiple subjects from different ethnic groups and gender. In contrast, the JAFFE dataset consists of only 10 Japanese female subjects, which imposes a large constraint on ethnicity and gender. This means that images in the JAFFE dataset will be equivalent to a small subset of the training images in the SFEW dataset. Consequently, this subset of SFEW images will contribute to a small training error but will produce a large test error on a test set, which has a distribution similar to it, in this case,

the JAFFE dataset.

Lastly, we compare the generalizability of the part-based ensemble and our two baseline networks. We observe that the full transfer learning network performs better than the baseline network, thereby highlighting the advantage of transfer learning from FLL to FER. Further, our proposed ensemble outperforms the full transfer learning network, demonstrating the benefit of a part-based ensemble over a 5-model ensemble of the full transfer learning network.

#### 4.4 Computational Complexity

In this section, we report the time and space complexity of inference. To report the worst-case complexities, we utilize the models trained on the CK+ dataset as they have the maximum number of parameters among the models trained on the three datasets. A single network of any type, baseline, full transfer learning, or ensemble transfer learning, has about **0.33M** parameters in the worst case (8 outputs of CK+ dataset). Similarly, the ensemble transfer learning network with five such models has about **1.65M** parameters and requires  **$3.28 \times 10^6$  FLOPS** in the worst case.

We calculate the inference time on the Nvidia Tesla K80 GPU and Intel(R) Xeon(R) CPU for all three networks. The inference time does not include time taken to load an image and a model, pre-process the image, detect a face in the image, and produce the 160x160x3 face crop input. A model of the baseline, full, or sub-network of the ensemble network takes **1.2 ms** to predict an image's expression on the GPU. Serial inferencing of the sub-networks of the ensemble model takes **6 ms** on average. Executing the ensemble policy, that is, summation and taking maximum, takes time in the order  $1 \times 10^{-4}$ ms, so we neglect it. Similarly, on the CPU, a model of the baseline, full, and sub-network of the ensemble transfer learning network takes **2.5 ms** to predict an image's expression and serial inferencing of the ensemble model's sub-networks takes **12.5 ms** on average.

Each model occupies approximately **5 MB** of space. Thus the ensemble transfer learning network consisting of five models occupies approximately **25 MB** of space.

### 5 DISCUSSION AND CONCLUSION

In this work, we propose a Part-based Ensemble Transfer Learning network, which models how humans recognize facial expressions. It correlates the spatial orientation pattern of the various facial features like eyebrows, eyes, nose, mouth, and jaw with a corresponding expression. The complementary nature of the ensemble sub-networks helps it achieve high classification accuracy that exceeds the benchmark for CK+ and JAFFE datasets. Additionally, the shallow sub-networks reduce model parameters, thereby ensuring computational efficiency for real-time deployment. Our proposed ensemble trained on the SFEW Train dataset demonstrates high cross-dataset generalization and obtains a higher test accuracy for the CK+ dataset than the SFEW Valid dataset itself.

We compare our sub-networks to the FACS Main Action Units and find out that they follow the same order of discriminability: mouth, eyes, eyebrows, jaw, and nose - with mouth having the highest and nose the lowest.

Here discriminability refers to the network's independent ability to classify expressions when it is not part of the ensemble. This shows that our proposed ensemble network learns visual patterns emanating from facial muscles' motor movements.

In all three datasets, we observe that transfer learning from facial landmark localization task to facial expression recognition leads to better classification accuracy than directly training the network to classify expression. The full transfer learning also performs better than the sub-networks of the proposed ensemble when they are considered individually. This is because the full transfer learning network pre-trains to learn all 68 fiducial points, whereas the sub-networks only learn a subset of those points, thereby reducing the patterns these sub-networks can learn independently. However, on combining the sub-networks in our proposed ensemble, they outperform the full transfer learning model across all three datasets and on both self and cross dataset evaluations. This validates the complementarity of the models, as redundant models would have produced an accuracy which is average of the five sub-models not greater than the highest accuracy achieved by one of the sub-model.

Furthermore, our part-based ensemble transfer learning network achieves ceiling level accuracy of **97.31%** on the CK+ dataset and **97.14%** on the JAFFE dataset (for the chosen evaluation policy) and outperforms the benchmark by **0.51%** and **5.34%** respectively. The proposed ensemble network approach is not only accurate but also computationally efficient. It has a total of **1.65M** model parameters that are lesser than the parameters of the current benchmark for all three datasets and requires only  **$3.28 \times 10^6$  FLOPS**. It has a worst-case inference time of **6 ms** on Nvidia Tesla K80 GPU and **12.5 ms** on Intel Xeon CPU. Moreover, it requires only **25 MB** of storage space in the worst case. We then perform Grad-CAM visualization for the baseline, full transfer learning, and our proposed ensemble learning network. Visualizations show that transfer learning helps the final classification model focus on the facial feature(s) for an accurate classification compared to the non-transfer learning baseline network. It also demonstrates that each sub-network of the part-based ensemble focuses on a specific facial feature for expression prediction, thereby strengthening the complementary nature of the sub-networks.

The Cross-dataset generalization tests reveal that generalizability is higher for transfer learning networks, with the highest for our part-based ensemble transfer learning network. Further, our proposed ensemble network trained on the SFEW Train dataset achieves a classification accuracy of **47.53%** on the CK+ dataset, which is higher than what it achieves on the SFEW Valid dataset. The generalization accuracy on the JAFFE dataset is comparatively low, owing to the significant constraint this dataset imposes on ethnicity and gender. Overall the generalizability of our proposed ensemble is high, with a scope of further improvement in the future.

Our trained models on the SFEW dataset show the same improvement pattern as in the CK+ and JAFFE datasets; that is, the proposed ensemble model performs the best and the baseline the worst. However, the proposed ensemble

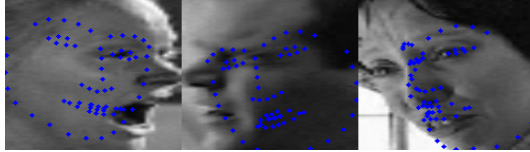


**Fig. 11:** Landmarks predicted by the ERT algorithm on the contrast-enhanced face crops used as input to the neural network. Each image is taken from the train set of the SFEW dataset and has a high magnitude of head pose angle.

model falls short of the current benchmark. We believe this is a limitation in learning an effective facial representation (feature vector). The feature extractor is primarily trained during the FLL phase. Only fine-tuning with a small learning rate is applied during the classification phase; thus, the facial representation is majorly learned during the FLL phase. During the FLL phase, the feature extractor learns a representation to minimize the error in predicting landmark positions. In the case of large errors in ground truth landmark positions, noise is likely to be introduced in the representation learned by the feature extractor. Thus, the expression classification model obtained by tuning this feature extractor will not be very accurate.

We visualized the ERT model used in our FER pipeline and observed that it made large mistakes in predicting landmark positions for SFEW images with extreme poses up to  $90^\circ$ , as shown in Fig. 11. As the ERT algorithm is used to create ground truth landmarks for the SFEW images, the annotated landmark positions and the corresponding facial features may be misaligned. This misalignment will induce noise in the facial representations learned by the network, and as a result, will reduce the expression prediction ability of the network. Thus, we are experimenting with more robust and accurate techniques for landmark ground-truth annotation. We also intend to explore the option of pre-training our proposed ensemble on the FER2013 dataset [5], a method used by recent works [52], [53]. Due to pre-training, the neural networks in these works have achieved accuracies north of 50% on the SFEW valid dataset. We also plan to evaluate the effect of pre-training on cross-dataset generalization tests.

Lastly, preliminary evaluations of all three networks - baseline, full transfer learning, and part-based ensemble learning network on the FER2013 train dataset- show that they are underfitting on the FER2013 test set. We believe this is due to the shallow networks employed in this paper. Therefore, we are progressively increasing the size of each network to ensure that high accuracy does not come at the cost of high computational complexity. Subsequently, we aim to test our proposed part-based ensemble transfer learning approach on FER2013, and RAF-DB [6] datasets.

## APPENDIX A IMAGE PRE-PROCESSING STAGES

### A.1 Image Contrast Enhancement

Each image, irrespective of the dataset, undergoes contrast enhancement. We experiment with different contrast enhancement techniques like Contrast Stretching (CS), Histogram Equalization (HE), and Contrast Limited

Adaptive Histogram Equalization (CLAHE) [38]. Contrast stretching improves the contrast in an image by stretching the range of intensity values it contains over a desired range of values by applying a linear scaling function to the image pixel values. Histogram Equalization computes a single histogram of intensities of an image in which it spreads out the most frequent intensity values of the image. Due to this, the intensities are better distributed, and the global contrast of the image increases. However, histogram equalization fails to capture local contrast and edge definition well. Adaptive Histogram Equalization (AHE) [54] improves upon HE by computing several histograms, each corresponding to a distinct section of the image. These histograms help redistribute the image's lightness values, thereby improving the local contrast and edge definition in each image region. CLAHE further improves AHE by preventing the over-amplification of noise that AHE may produce in the image's near-constant regions. We test these methods' suitability in terms of the number of missed or incorrect face detections when the corresponding contrast enhancement technique is applied, keeping the face detection algorithm constant, as shown in Fig. 12a. The experiments reveal no missed or incorrect detections in the CK+ and JAFFE dataset, irrespective of the technique. However, the differentiator is the SFEW dataset. We observe that the face detector fails to detect specific images due to the variable contrast in the SFEW dataset's images. CLAHE performs the best out of the three, followed by contrast stretching between the 2nd and 98th percentile of images and histogram equalization in the respective order. Therefore, we use CLAHE to perform contrast enhancement of all images across all three datasets.

### A.2 Face Detection

After contrast enhancement of an image, we apply the face detector and take a detected facial region crop. For this purpose, we experiment with three face detectors with open-source implementation, namely - Viola-Jones HaarCascade face detector [55], Histogram of Gradients (HOG) face detector [56], and Single Shot Multibox Detector (SSD) [39]. We use the OpenCV [40] implementation of the Haar Cascade detector, the Dlib [57] implementation of the HoG detector trained on 2825 images from the Labeled Faces in the Wild (LFW) dataset [58], and OpenCV's SSD detector's implementation trained on face images from the web. We analyze their performance on the three datasets, as shown in Fig. 12b. The three detectors can detect a face in all the CK+ and JAFFE dataset images, with variation in only the detected facial region. However, we observe failure in detection or false detection in the images of the SFEW dataset. This can again be attributed to the varied head poses, facial size, and contrast in the SFEW images. On the other hand, the images in CK+ and JAFFE dataset all have frontal poses without rotation, similar facial sizes, and lab-controlled consistent illumination. Among the detectors, the SSD face detector has the least missed or incorrect detections in SFEW images, and it also detects faces in all the images in the CK+ and JAFFE datasets. SSD is able to detect faces at various head pose angles, as shown in Fig. 12b. Therefore, we incorporate the SSD face detector in our FER pipeline.



**(a)** Comparing the three different contrast enhancement techniques on the three datasets' images, keeping the same face detection algorithm, that is, the Single Shot Multibox Detector. From top-to-bottom: Contrast Stretching, Histogram Equalization, Contrast Limited Adaptive Histogram Equalization. From Left-to-Right: CK+, JAFFE, SFEW Dataset, respectively.

**(b)** Comparing the three different face detection techniques. Here each input image is taken from the SFEW and contrast-enhanced using CLAHE before feeding it to the detector. From top-to-bottom: Haar Cascade Detector, Histogram of Gradients Detector, Single Shot Detector. From Left-to-Right: Increase in the magnitude of head pose angle.

**(c)** Comparison between ERT and LBF face landmark localization technique. Here the images are taken from the SFEW dataset, and the top row represents images with ERT, and the bottom with LBF face landmark localization, respectively.

**Fig. 12**

### A.3 Landmarks Localization

We experiment with various landmark algorithms with open-source implementations, like Ensemble Regression of Trees (ERT) [44] and Local Binary Features (LBF) regression [59]. We start by applying these algorithms to the facial crops produced after face detection. Then, we evaluate an FLL model's performance based on the absolute difference between the landmark position predicted in the face crops and the corresponding ground truth position provided in CK+ and SFEW dataset. On comparing the performance, we found that ERT performs better than LBF in the SFEW dataset (shown in Fig. 12c), whereas both perform equally well in the CK+ dataset. Therefore, we use the ERT algorithm to generate ground truth labels for the FLL task.

### ACKNOWLEDGMENTS

The work is supported by MeitY(Government of India) under grant 4(16)/2019-ITEA.

### REFERENCES

- [1] P. Lucey, J. F. Cohn, T. Kanade, J. Saragih, Z. Ambadar, and I. Matthews, "The extended cohn-kanade dataset (ck+): A complete dataset for action unit and emotion-specified expression," in *2010 IEEE Computer Society Conference on Computer Vision and Pattern Recognition - Workshops*, 2010, pp. 94–101.
- [2] M. Lyons, S. Akamatsu, M. Kamachi, and J. Gyoba, "Coding facial expressions with gabor wavelets," in *Proceedings Third IEEE international conference on automatic face and gesture recognition*. IEEE, 1998, pp. 200–205.
- [3] A. Dhall, R. Goecke, S. Lucey, and T. Gedeon, "Static facial expression analysis in tough conditions: Data, evaluation protocol and benchmark," in *2011 IEEE International Conference on Computer Vision Workshops (ICCV Workshops)*, 2011, pp. 2106–2112.
- [4] A. Dhall, R. Goecke, S. Lucey, and T. Gedeon, "Collecting large, richly annotated facial-expression databases from movies," *IEEE multimedia*, no. 3, pp. 34–41, 2012.
- [5] I. J. Goodfellow, D. Erhan, P. L. Carrier, A. Courville, M. Mirza, B. Hamner, W. Cukierski, Y. Tang, D. Thaler, D.-H. Lee *et al.*, "Challenges in representation learning: A report on three machine learning contests," in *International conference on neural information processing*. Springer, 2013, pp. 117–124.
- [6] S. Li, W. Deng, and J. Du, "Reliable crowdsourcing and deep locality-preserving learning for expression recognition in the wild," in *2017 IEEE Conference on Computer Vision and Pattern Recognition (CVPR)*. IEEE, 2017, pp. 2584–2593.
- [7] A. Krizhevsky, I. Sutskever, and G. E. Hinton, "Imagenet classification with deep convolutional neural networks," in *Advances in neural information processing systems*, 2012, pp. 1097–1105.
- [8] K. Simonyan and A. Zisserman, "Very deep convolutional networks for large-scale image recognition," *arXiv preprint arXiv:1409.1556*, 2014.
- [9] C. Szegedy, W. Liu, Y. Jia, P. Sermanet, S. Reed, D. Anguelov, D. Erhan, V. Vanhoucke, and A. Rabinovich, "Going deeper with convolutions," in *Proceedings of the IEEE conference on computer vision and pattern recognition*, 2015, pp. 1–9.
- [10] H.-W. Ng, V. D. Nguyen, V. Vonikakis, and S. Winkler, "Deep learning for emotion recognition on small datasets using transfer learning," in *Proceedings of the 2015 ACM on International Conference on Multimodal Interaction*. Association for Computing Machinery, 2015, p. 443–449.
- [11] H. Ding, S. K. Zhou, and R. Chellappa, "Facenet2expnet: Regularizing a deep face recognition net for expression recognition," in *2017 12th IEEE international conference on automatic face & gesture recognition (FG 2017)*. IEEE, 2017, pp. 118–126.
- [12] Y. Guo, L. Zhang, Y. Hu, X. He, and J. Gao, "Ms-celeb-1m: A dataset and benchmark for large-scale face recognition," in *European conference on computer vision*. Springer, 2016, pp. 87–102.
- [13] Q. Cao, L. Shen, W. Xie, O. M. Parkhi, and A. Zisserman, "Vggface2: A dataset for recognising faces across pose and age," in *2018 13th IEEE International Conference on Automatic Face & Gesture Recognition (FG 2018)*. IEEE, 2018, pp. 67–74.
- [14] D. Yi, Z. Lei, S. Liao, and S. Z. Li, "Learning face representation from scratch," *arXiv preprint arXiv:1411.7923*, 2014.
- [15] H. Kaya, F. Gürpınar, and A. A. Salah, "Video-based emotion recognition in the wild using deep transfer learning and score fusion," *Image and Vision Computing*, vol. 65, pp. 66–75, 2017.
- [16] S. E. Kahou, C. Pal, X. Bouthillier, P. Froumenty, Ç. Gülcühre, R. Memisevic, P. Vincent, A. Courville, Y. Bengio, R. C. Ferrari *et al.*, "Combining modality specific deep neural networks for emotion recognition in video," in *Proceedings of the 15th ACM on International conference on multimodal interaction*, 2013, pp. 543–550.
- [17] B.-K. Kim, H. Lee, J. Roh, and S.-Y. Lee, "Hierarchical committee of deep cnns with exponentially-weighted decision fusion for static facial expression recognition," in *Proceedings of the 2015 ACM on International Conference on Multimodal Interaction*, 2015, p. 427–434.
- [18] Z. Yu and C. Zhang, "Image based static facial expression recognition with multiple deep network learning," in *Proceedings of the 2015 ACM on International Conference on Multimodal Interaction*. Association for Computing Machinery, 2015, p. 435–442.
- [19] G. Pons and D. Masip, "Supervised committee of convolutional neural networks in automated facial expression analysis," *IEEE Transactions on Affective Computing*, vol. 9, no. 3, pp. 343–350, 2017.
- [20] T. Devries, K. Biswaranjan, and G. W. Taylor, "Multi-task learning of facial landmarks and expression," in *2014 Canadian Conference on Computer and Robot Vision*. IEEE, 2014, pp. 98–103.
- [21] K. Zhang, Y. Huang, Y. Du, and L. Wang, "Facial expression recognition based on deep evolutionary spatial-temporal networks," *IEEE Transactions on Image Processing*, vol. 26, no. 9, pp. 4193–4203, 2017.
- [22] G. Pons and D. Masip, "Multi-task, multi-label and multi-domain learning with residual convolutional networks for emotion recognition," *arXiv preprint arXiv:1802.06664*, 2018.

[23] R. Ekman, *What the face reveals: Basic and applied studies of spontaneous expression using the Facial Action Coding System (FACS)*. Oxford University Press, USA, 1997.

[24] R. R. Selvaraju, M. Cogswell, A. Das, R. Vedantam, D. Parikh, and D. Batra, "Grad-cam: Visual explanations from deep networks via gradient-based localization," in *Proceedings of the IEEE international conference on computer vision*, 2017, pp. 618–626.

[25] P. Liu, S. Han, Z. Meng, and Y. Tong, "Facial expression recognition via a boosted deep belief network," in *2014 IEEE Conference on Computer Vision and Pattern Recognition*, 2014, pp. 1805–1812.

[26] Mengyi Liu, Shaoxin Li, Shiguang Shan, and Xilin Chen, "Au-aware deep networks for facial expression recognition," in *2013 10th IEEE International Conference and Workshops on Automatic Face and Gesture Recognition (FG)*, 2013, pp. 1–6.

[27] M. Liu, S. Li, S. Shan, and X. Chen, "Au-inspired deep networks for facial expression feature learning," *Neurocomput.*, vol. 159, no. C, p. 126–136, 2015.

[28] P. Khorrami, T. Paine, and T. Huang, "Do deep neural networks learn facial action units when doing expression recognition?" in *Proceedings of the IEEE International Conference on Computer Vision Workshops*, 2015, pp. 19–27.

[29] F. Cheng, J. Yu, and H. Xiong, "Facial expression recognition in jaffe dataset based on gaussian process classification," *IEEE Transactions on Neural Networks*, vol. 21, no. 10, pp. 1685–1690, 2010.

[30] M. Kyperountas, A. Tefas, and I. Pitas, "Salient feature and reliable classifier selection for facial expression classification," *Pattern Recognition*, vol. 43, no. 3, pp. 972–986, 2010.

[31] D. Liang, J. Yang, Z. Zheng, and Y. Chang, "A facial expression recognition system based on supervised locally linear embedding," *Pattern Recognition Letters*, vol. 26, no. 15, pp. 2374–2389, 2005.

[32] C. Shan, S. Gong, and P. W. McOwan, "Facial expression recognition based on local binary patterns: A comprehensive study," *Image and vision Computing*, vol. 27, no. 6, pp. 803–816, 2009.

[33] M. Dahmane and J. Meunier, "Prototype-based modeling for facial expression analysis," *IEEE Transactions on Multimedia*, vol. 16, no. 6, pp. 1574–1584, 2014.

[34] A. Dhall, O. Ramana Murthy, R. Goecke, J. Joshi, and T. Gedeon, "Video and image based emotion recognition challenges in the wild: Emotiw 2015," in *Proceedings of the 2015 ACM on international conference on multimodal interaction*, 2015, pp. 423–426.

[35] M. Liu, S. Shan, R. Wang, and X. Chen, "Learning expressionlets on spatio-temporal manifold for dynamic facial expression recognition," in *Proceedings of the IEEE conference on computer vision and pattern recognition*, 2014, pp. 1749–1756.

[36] A. Mollahosseini, D. Chan, and M. H. Mahoor, "Going deeper in facial expression recognition using deep neural networks," in *2016 IEEE Winter conference on applications of computer vision (WACV)*. IEEE, 2016, pp. 1–10.

[37] G. Levi and T. Hassner, "Emotion recognition in the wild via convolutional neural networks and mapped binary patterns," in *Proceedings of the 2015 ACM on international conference on multimodal interaction*, 2015, pp. 503–510.

[38] K. Zuiderveld, *Contrast Limited Adaptive Histogram Equalization*. USA: Academic Press Professional, Inc., 1994, p. 474–485.

[39] W. Liu, D. Anguelov, D. Erhan, C. Szegedy, S. Reed, C.-Y. Fu, and A. C. Berg, "Ssd: Single shot multibox detector," in *European conference on computer vision*. Springer, 2016, pp. 21–37.

[40] G. Bradski, "The OpenCV Library," *Dr. Dobb's Journal of Software Tools*, 2000.

[41] T. F. Cootes, G. J. Edwards, and C. J. Taylor, "Active appearance models," *IEEE Transactions on pattern analysis and machine intelligence*, vol. 23, no. 6, pp. 681–685, 2001.

[42] I. Matthews and S. Baker, "Active appearance models revisited," *International journal of computer vision*, vol. 60, no. 2, pp. 135–164, 2004.

[43] J. Saragih and R. Göcke, "Learning aam fitting through simulation," *Pattern Recognition*, vol. 42, no. 11, pp. 2628–2636, 2009.

[44] V. Kazemi and J. Sullivan, "One millisecond face alignment with an ensemble of regression trees," in *Proceedings of the IEEE conference on computer vision and pattern recognition*, 2014, pp. 1867–1874.

[45] C. Sagonas, E. Antonakos, G. Tzimiropoulos, S. Zafeiriou, and M. Pantic, "300 faces in-the-wild challenge: Database and results," *Image and vision computing*, vol. 47, pp. 3–18, 2016.

[46] A. F. Agarap, "Deep learning using rectified linear units (relu)," *arXiv preprint arXiv:1803.08375*, 2018.

[47] S. Ioffe and C. Szegedy, "Batch normalization: Accelerating deep network training by reducing internal covariate shift," *arXiv preprint arXiv:1502.03167*, 2015.

[48] K. He, X. Zhang, S. Ren, and J. Sun, "Delving deep into rectifiers: Surpassing human-level performance on imagenet classification," in *Proceedings of the IEEE international conference on computer vision*, 2015, pp. 1026–1034.

[49] X. Glorot and Y. Bengio, "Understanding the difficulty of training deep feedforward neural networks," in *Proceedings of the thirteenth international conference on artificial intelligence and statistics*, 2010, pp. 249–256.

[50] D. P. Kingma and J. Ba, "Adam: A method for stochastic optimization," *arXiv preprint arXiv:1412.6980*, 2014.

[51] S. Li and W. Deng, "Deep facial expression recognition: A survey," *IEEE Transactions on Affective Computing*, 2020.

[52] X. Liu, B. V. K. V. Kumar, J. You, and P. Jia, "Adaptive deep metric learning for identity-aware facial expression recognition," in *2017 IEEE Conference on Computer Vision and Pattern Recognition Workshops (CVPRW)*, 2017, pp. 522–531.

[53] J. Cai, Z. Meng, A. S. Khan, Z. Li, J. O'Reilly, and Y. Tong, "Island loss for learning discriminative features in facial expression recognition," in *2018 13th IEEE International Conference on Automatic Face & Gesture Recognition (FG 2018)*. IEEE, 2018, pp. 302–309.

[54] S. Pizer, E. P. Amburn, J. D. Austin, R. Cromartie, A. Geselowitz, T. Greer, B. T. H. Romeny, and J. B. Zimmerman, "Adaptive histogram equalization and its variations," *Graphical Models graphical Models and Image Processing computer Vision, Graphics, and Image Processing*, vol. 39, pp. 355–368, 1987.

[55] P. Viola and M. Jones, "Rapid object detection using a boosted cascade of simple features," in *Proceedings of the 2001 IEEE computer society conference on computer vision and pattern recognition. CVPR 2001*, vol. 1. IEEE, 2001, pp. I–I.

[56] N. Dalal and B. Triggs, "Histograms of oriented gradients for human detection," in *2005 IEEE computer society conference on computer vision and pattern recognition (CVPR'05)*, vol. 1. IEEE, 2005, pp. 886–893.

[57] D. E. King, "Dlib-ml: A machine learning toolkit," *Journal of Machine Learning Research*, vol. 10, pp. 1755–1758, 2009.

[58] G. B. Huang, M. Mattar, T. Berg, and E. Learned-Miller, "Labeled faces in the wild: A database for studying face recognition in unconstrained environments," 2008.

[59] S. Ren, X. Cao, Y. Wei, and J. Sun, "Face alignment at 3000 fps via regressing local binary features," in *Proceedings of the IEEE Conference on Computer Vision and Pattern Recognition*, 2014, pp. 1685–1692.



the URL: <http://www.rohanwadhawan.com>

**Rohan Wadhawan** (Student Member, IEEE) is a Research Assistant with the Department of Electrical Engineering, IIT Delhi, India. He is pursuing B.E. in Computer Engineering at Netaji Subhas Institute of Technology, University of Delhi, India and is expected to graduate by November 2020. His research interests include machine learning, computer vision, affective computing, face detection, recognition and generation, and assistive technology. The detailed biographical information can be found at



**Tapan K. Gandhi** (Senior Member, IEEE) is an Associate Professor with the Department of Electrical Engineering, IIT Delhi, India. Prior to joining IIT Delhi as a Faculty Member, he was a Postdoctoral Fellow with the Massachusetts Institute of Technology (MIT), Cambridge, USA. He received his B.Sc. degree in physics, an M.Sc. degree in electronics, the M.Tech. Degree in bioelectronics, and a Ph.D. degree in biomedical engineering from IIT Delhi in 2001, 2003, 2006, and 2011, respectively. His research interests include computational neuroscience, artificial intelligence, medical instrumentation, biomedical signal and image processing, and assistive technology. The detailed biographical information can be found at the URL: <https://tapankgandhi.com/>